Estimation of acoustically induced refractive index perturbation in silicon and germanium slab for optical applications

Gaurav SHARMA, Sushil KUMAR, Dinesh KUMAR, Vivek SINGH[*]

Department of Physics, Faculty of Science, Banaras Hindu University,
Varanasi, UP 221005, India

[*]Corresponding author: viveks@bhu.ac.in

In-plane displacement field and refractive index variation for silicon and germanium in the presence of Lamb wave is estimated for optical applications. The required dispersion equation in a thin silicon and germanium plates is obtained using the method of potentials with boundary conditions involving the bulk and surface stress of the materials considered. The eigen-values thus obtained are used to compute the Lamb wave modes for the slab of silicon and germanium at same thickness. The fundamental anti-symmetric and symmetric plate modes and their overtones are observed due to confinement of acoustic energy within the slab thickness. In addition, the excited symmetric modes in silicon have longer wavelengths than those of germanium at a fixed frequency. Therefore, the refractive index modulation through the Lamb wave in silicon is always larger as compared to that of germanium. This refractive index modulation can be treated as periodic sinusoidal refractive index variation and may be considered as a tunable one-dimensional photonics crystal.

Keywords: dispersion relation, Lamb wave mode in silicon and germanium, displacement field, refractive index modulation.

1. Introduction

Light is used in a variety of devices and instruments in modern times such as to sense, process and store information *etc*. On the other hand, the application of photonics band gap (PBG) materials has drawn much attraction in recent years [1]. The working status of many optical devices based on PBG, such as optical modulators [2], optical filters [3], and optical biosensors [4] is dependent on the refractive index modulation of such artificial materials during operation. Refractive index (RI) of the light propagating in a medium is a most fundamental property; and materials with dynamic control of RI may be able to create devices like tuneable filters, shutter, attenuate, phase shift optical signals *etc*. Active control of modulation in RI of submicron dielectric films is the keystone in photonic crystal-based devices. Acoustic modes modulate dielectric constants

in both the spatial and time domains of dielectric media so that polarization and intensity of light can be manipulated through the acousto-optic (AO) effect [5]. Acoustic waves with frequencies in the range from hundreds of megahertz to several gigahertz can be generated by piezoelectric thin-film transducers, or electrostatic forces in microstructures [6, 7]. Propagation of bulk and surface acoustic waves in such different structures has attracted a lot of interest due to their renewed physical properties. Acoustic waves are confined by the two free surfaces of the plates, what results in surface characterized modes only, called Lamb waves, that were discovered by Horace Lamb in 1917. The Lamb waves are two-dimensional vibrations propagating in plates with free boundary conditions and possess some fascinating properties in isotropic and anisotropic plates [8]. The Lamb waves can propagate over a long distance in metals sheets, dielectric slabs and also in materials with a high attenuation ratio like carbon fibre-reinforced composites *etc*. These waves can be used to achieve an enhanced modulation of RI for dynamic control of the photonic structures by acoustic wave energy and open the possibility of tuneable optical devices. Tuneable optical devices have drawn much attention of many researchers in recent years due to their various possible applications in optics-based lab-on-a-chip systems. Recent developments in photonics have demonstrated the possibility of controlling optical energy in compact and highly integrated micro- and nano-scale devices, which provide promising applications for the next generation of photonics technology [9–11].

However, certain materials like silicon and germanium show strain induced energy band gap shrinkage [12] which may be exploited in the design of tuneable optical devices. An experimental study on the shrinkage of indirect bandgap of silicon on insulator shows good agreement with the theoretical calculation [13]. The acoustic plate waves generate a displacement field that causes the motion of the interfaces as well as a strain field that changes the refractive index (bulk effect) of the dielectric slab [14]. These effects modulate the guided optical waves having a reduced group velocity; and in turn, it enhances the AO interaction.

Moreover, the change in RI through strain is a bio-inspired phenomenon. It is found that many chameleons and panther chameleons have the remarkable ability to exhibit complex and rapid colour changes due to the strain produced on their skin under various circumstances [15]. In practice the optical loss in Ge is less than 2 dB/cm for a wide range of wavelength (2–14 μm) and its unperturbed refractive index is approximately 4 while for Si this range is only 1–10 μm and unperturbed refractive index is approximately 3.4 [16]. Therefore, for a wide range of optical applications, Ge seems to be a good material in comparison with Si. Hence, in the present communication we considered two semiconductor materials Ge and Si which are widely used in electronic networks and we estimated their maximum possible index variations at the fixed acoustic frequency for optical applications which were ignored in previous studies [17]. The effect of acoustic strain on silicon and germanium slabs that shows a promising method to control the RI in such structures can be used in the design of tuneable optical devices. Since velocity of acoustic waves is five orders of magnitude smaller than that of optical waves, the characteristic time scale of the time varying strain field is much

longer than the time period for optical waves. Therefore, acoustic modes can be treated as quasi-static perturbations to the propagation of light during AO interaction [18].

2. Model and computational approach

Elastic waves in solid media are guided by the boundaries of the media in which they propagate. Let us consider harmonic wave propagation in a thin slab having thickness 2h as shown in Fig. 1.
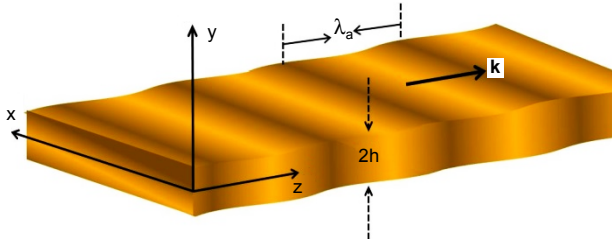

Fig. 1. Schematic diagram of the acoustically perturbed dielectric slab, where z is the direction of propagation of acoustic wave and 2h is unperturbed slab thickness along y-direction.

Since the considered material is a thin silicon plate, therefore the method of potentials with boundary conditions, which rapidly leads to the dispersion relation for isotropic plates, is used. The displacement u of the material can be derived from a scalar potential ϕ and a vector potential $\boldsymbol{\psi}$, so that

$$u = \nabla\phi + \nabla \times \boldsymbol{\psi} \tag{1}$$

and the potentials satisfy the wave equations

$$\nabla^2\phi - \frac{1}{V_L^2}\frac{\partial^2\phi}{\partial t^2} = 0 \tag{2a}$$

$$\nabla^2\boldsymbol{\psi} - \frac{1}{V_T^2}\frac{\partial^2\boldsymbol{\psi}}{\partial t^2} = 0 \tag{2b}$$

where $\nabla^2 = \partial^2/\partial x^2 + \partial^2/\partial y^2 + \partial^2/\partial z^2$, and V_L and V_T are the phase velocities of bulk longitudinal and transverse waves, respectively. In Cartesian coordinates $\boldsymbol{\psi} = [\psi_x, \psi_y, \psi_z]$ and the Helmholtz displacement decomposition will have the form $u_x = \partial\psi_y/\partial z + \partial\psi_z/\partial x - \partial\psi_x/\partial y$, $u_y = \partial\phi/\partial y - \partial\psi_z/\partial x + \partial\psi_x/\partial z$ and $u_z = \partial\phi/\partial x + \partial\psi_z/\partial y - \partial\psi_y/\partial z$.

Strains associated with dilatation, causing volume changes, are expressed by ϕ and shear strains, causing no volume changes, are expressed by $\boldsymbol{\psi}$. Here the Lamb wave is taken to propagate along z-direction, therefore the wave propagation vector **k** is along z-direction. The diffraction of the Lamb wave in x-direction is ignored by choosing

$\partial/\partial x = 0$. For the sinusoidal variation we can consider $\partial/\partial z = -ik$. Considering these assumptions, the Laplacian equation for function ϕ and $\psi \equiv \psi_z$ can be written as

$$\frac{\partial^2 \phi}{\partial y^2} + p^2 \phi = 0 \tag{3a}$$

$$\frac{\partial^2 \psi}{\partial y^2} + q^2 \psi = 0 \tag{3b}$$

where $p^2 = \omega^2/V_L^2 - k^2$ and $q^2 = \omega^2/V_T^2 - k^2$.

The solution of the above equations can be simplified by determining the null stress boundary condition at the faces $y = \pm h$ and by applying symmetry motion conditions. The cosine motion of u_z is called symmetric and the sine motion of u_z is called anti-symmetric with respect to $y = 0$ for u_z in the yz plane; for u_y it is *vice versa*. Hence, the modes of wave propagation in the considered thin plate may be separated into following two systems of symmetric and antisymmetric modes: $\phi = B\cos(py + \alpha)$ and $\psi = A\sin(qy + \alpha)$ where $\alpha = 0$ or $\alpha = \pi/2$.

There are two types of Lamb waves; first is a symmetric Lamb wave ($\alpha = 0$) on either side of the median plane where the longitudinal components are equal and the transverse components are opposite; and second is an antisymmetric Lamb wave ($\alpha = \pi/2$) on either side of the median plane where the transverse components are equal and the longitudinal components are opposite. The solution of the above equation in the form of mechanical displacements is given as [19]

$$u_y = ikA\left[\sin(qy + \alpha) + \frac{2pq}{k^2 - q^2}\frac{\cos(qh + \alpha)}{\cos(ph + \alpha)}\sin(py + \alpha)\right]\exp[i(\omega t - kz)] \tag{4a}$$

$$u_z = qA\left[\cos(qy + \alpha) - \frac{2k^2}{k^2 - q^2}\frac{\cos(qh + \alpha)}{\cos(ph + \alpha)}\cos(py + \alpha)\right]\exp[i(\omega t - kz)] \tag{4b}$$

where ω is the frequency and k is the wave number. These solutions represent traveling waves in the z-direction and standing waves in the y-direction. The frequency equation can be obtained from the boundary conditions. The frequency equation for symmetric case ($\alpha = 0$) of considered plate of thickness $2h$ having traction free boundaries can be written as

$$\begin{bmatrix} (k^2 - q^2)\cos(ph) & 2kq\cos(qh) \\ \mp 2ikp\sin(ph) & \mp(k^2 - q^2)\sin(qh) \end{bmatrix}\begin{bmatrix} B \\ A \end{bmatrix} = \begin{bmatrix} 0 \\ 0 \end{bmatrix} \tag{5}$$

Since the system of Eq. (5) is homogeneous, therefore the determinant of the coefficients has to vanish, which results in the frequency equation

$$(k^2 - q^2)^2 \cos(ph)\sin(qh) + 4k^2 pq \sin(ph)\cos(qh) = 0 \tag{6a}$$

The determinant can be written as

$$\frac{\tan(qh)}{\tan(ph)} = -\frac{4k^2 pq}{(k^2 - q^2)^2} \tag{6b}$$

Equation (6b) is known as the Rayleigh–Lamb frequency equation for symmetric waves in a plate. Using the similar steps for antisymmetric modes ($\alpha = \pi/2$) the following system for constants A and B is obtained and results in the frequency equation

$$2kpB\cos(ph) - (k^2 - q^2)A\cos(qh) = 0 \tag{7a}$$

This gives the relation known as the Rayleigh–Lamb frequency equation for antisymmetric waves in a plate:

$$\frac{\tan(qh)}{\tan(ph)} = -\frac{(k^2 - q^2)^2}{4k^2 pq} \tag{7b}$$

These relations state the dispersion relations between the frequencies and the wave numbers and yield an infinite number of branches for an infinite number of symmetric and antisymmetric modes. The symmetric modes can be considered as longitudinal modes because the average displacement over the thickness is in that direction. The antisymmetric modes are generally termed the flexural modes since the average displacement is in the transverse direction. When acoustic energy completely confines within the slab thickness, there are fundamental antisymmetric and symmetric (A_0 and S_0) plate modes and their overtones (A_n and S_n, $n = 1, 2, 3, \ldots$) are observed. The A_0, S_0, A_1, S_1 modes are mostly applied acoustic plate modes because they are easier to excite and also have a simple displacement profile. Here, we consider the fundamental plate modes and frequency corresponding to the submicron wavelengths [20]. Travelling acoustic waves along the z-direction in the slab generate deformation that is represented by the displacement value u and hence there is a strain field, *i.e.*, partial derivative of the displacement field. In-plane displacement fields of the acoustic eigenmodes u_y and u_z are governed by the following coupled stress-wave equations:

$$\frac{\partial}{\partial y}\left(c_{11}\frac{\partial u_y}{\partial y} + c_{12}\frac{\partial u_z}{\partial z}\right) + \frac{\partial}{\partial z}\left(c_{44}\frac{\partial u_y}{\partial z} + c_{44}\frac{\partial u_z}{\partial y}\right) = \rho\frac{\partial^2 u_y}{\partial t^2} \tag{8a}$$

$$\frac{\partial}{\partial z}\left(c_{11}\frac{\partial u_z}{\partial z} + c_{12}\frac{\partial u_y}{\partial y}\right) + \frac{\partial}{\partial y}\left(c_{44}\frac{\partial u_y}{\partial y} + c_{44}\frac{\partial u_y}{\partial z}\right) = \rho\frac{\partial^2 u_z}{\partial t^2} \tag{8b}$$

where c_{11}, c_{12} are the two independent elastic stiffness constants, $c_{44} = c_{11} - c_{12}/2$ depends on the c_{11} and c_{12}, and ρ is the mass density. In Equations (4a) and (4b), A represents the maximum displacement amplitude. This displacement and strain produce variations of the air slab interfaces and vary from time-to-time along with the acoustic wave propagation. Some parts of the slab are shrunk while other parts may expand due to the propagation of acoustic waves at a certain moment, which would induce refractive index variation. This acoustically induced strain field changes the refractive indices of the slab due to the photoelastic effect. The photoelastic effect relates to the change of the refractive index Δn_{ij} in the strained structure that can be computed according to the photoelastic relation [3]

$$\Delta n_{yy} = -\frac{1}{2}n^3\left(p_{11}\frac{\partial u_y}{\partial y} + p_{12}\frac{\partial u_z}{\partial z}\right) \tag{9a}$$

$$\Delta n_{zz} = -\frac{1}{2}n^3\left(p_{12}\frac{\partial u_y}{\partial y} + p_{11}\frac{\partial u_z}{\partial z}\right) \tag{9b}$$

where p_{11} and p_{12} are strain-optic coefficients and n is the refractive index of an unstrained slab waveguide.

3. Numerical results and discussion

Now we are in position to compute the in-plane displacement field and variation of the refractive index for both silicon and germanium plates. To excite the fundamental and first over-tone of a symmetric mode in Si and Ge slabs simultaneously, the acoustic frequency 5 GHz is selected. The corresponding wavelengths for two symmetric acoustic eigenmodes in Si slab are obtained at λ_a = 1185 and 1683 nm, as shown in Fig. 2**a**. Similarly, the two symmetric acoustic eigenmodes in the Ge slab are obtained at λ_a = 625 and 1537 nm, as shown in Fig. 2**b**.

Figures 2**a** and 2**b** show the dispersion curves of the some lowest in-plane (yz plane) acoustic plate waves in the Si and Ge slab of thickness 500 nm, respectively. The slopes of dispersion curves for Si slab (Fig. 2**a**), are very steep in comparison with that of Ge slab (Fig. 2**b**). The Si slab supports the lower number of acoustic plate modes at the same thickness due to its higher phase velocities of bulk longitudinal and transverse waves. Also, the group velocity of the second symmetric mode S_1 of Si slab in the frequency range 4.04–4.24 GHz and symmetric modes S_0 and S_2 of Ge slab in the frequency range 2.37–2.53 GHz and 6.9–7.1 GHz, respectively, become negative. This shows
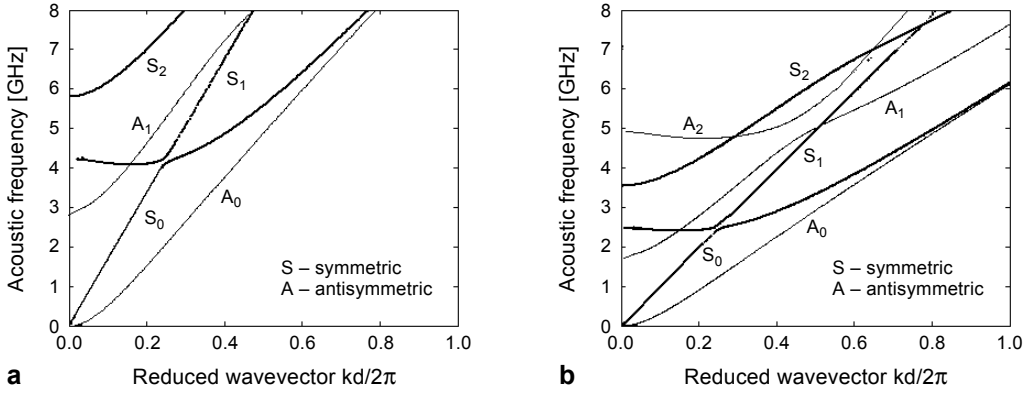
Fig. 2. Dispersion curves of some lowest in-plane acoustic modes for Si (**a**) and for Ge (**b**).
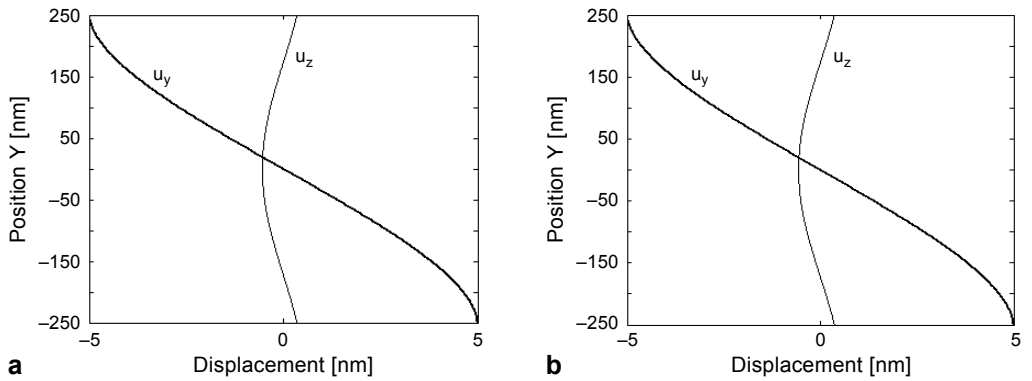

Fig. 3. Displacement fields of the lowest symmetric acoustic eigenmodes at acoustic frequency at 5 GHz in Si (**a**) and in Ge (**b**).

that in these frequency ranges, these materials may exhibit the property of negative index for guided elastic waves in isotropic media. To understand the refractive index modulation in such structures, the in-plane mechanical displacement fields (u_y and u_z) of a fundamental symmetric mode in Si and Ge plates are shown in Fig. 3.

Here both plots of Si slab and Ge slab are almost the same because the maximum acceptable displacement in the *y*-direction is 1% of the slab thickness (5 nm); and in the *z*-direction, it is limited by the lattice constant. The lattice constant of Si and Ge are 0.543 and 0.565 nm, respectively [5]. Here the variation in displacement fields, hence strain fields, are responsible for refractive index variation in the corresponding direction.

Figures 4 and 5 show the change in the RI due to the propagation of symmetric Lamb wave modes in Si slab and Ge slab, respectively. The sinusoidal index variation
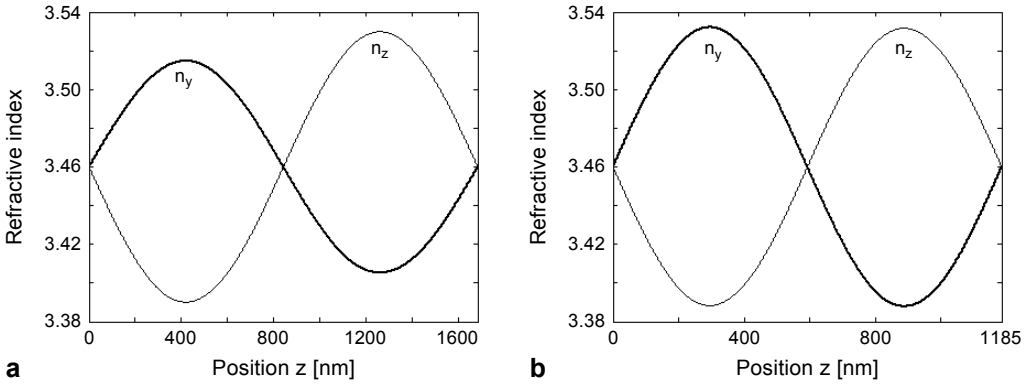
Fig. 4. Variation in the refractive index of Si for S_0 (**a**) and for S_1 (**b**) symmetric acoustic eigenmodes at acoustic frequency 5 GHz
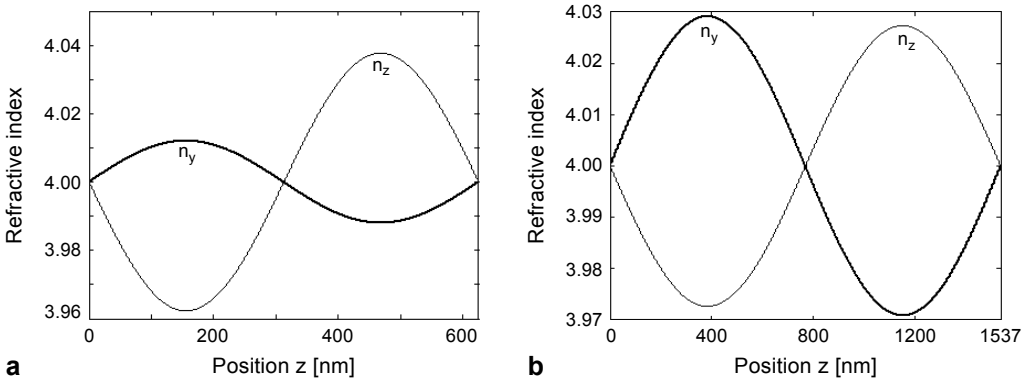

Fig. 5. Variation in the refractive index of Ge for S_0 (**a**) and for S_1 (**b**) symmetric acoustic eigenmodes at acoustic frequency 5 GHz.

is observed in both *y*- and *z*-directions. In Si plate, observed refractive index variation for fundamental symmetric mode (S_0) is larger than its first overtone (S_1). The observed RI modulations for the two lowest modes in Si and Ge plates are calculated and tabulated in Table 1. It is clear from the table that maximum RI variations considered are 0.160 and 0.072 along the *z*-direction in Si and Ge plates, respectively. Since the excited modes in Si slab have larger wavelengths (1185 and 1683 nm) as compared with those of Ge slab (625 and 1537 nm) at the chosen frequency 5 GHz, the observed RI

T a b l e 1. Maximum index variations for two lowest Lamb wave modes.

Symmetric Lamb modes	Silicon (unperturbed RI = 3.46)		Germanium (unperturbed RI = 4.00)	
	Δn_y	Δn_z	Δn_y	Δn_z
S_0	0.144	0.160	0.036	0.072
S_1	0.110	0.140	0.058	0.054

contrast in Si plate is always higher than that of Ge plate. Also, these exited modes lie within near-infrared region where both materials exhibit low propagation loss [16], therefore, the possible applications of these materials are in the design of tuneable photonic crystal-based optical devices in near-infrared region.

4. Conclusions

The refractive index modulations in Si slab and Ge slab are achieved by the propagation of Lamb wave in dielectric materials. It was observed that these materials are found to exhibit the property of negative index for elastic waves in isotropic media in certain frequency range. The observed index modulation in Si slab is larger than that of Ge slab. This index modulation is highly effected by the elastic stiffness constant of the materials.

References

[1] PAVESI L., LOCKWOOD D., *Silicon Photonics*, Springer-Verlag, 2004.

[2] ANSHENG LIU, LING LIAO, RUBIN D., HAT NGUYEN, CIFTCIOGLU B., CHETRIT Y., IZHAKY N., PANICCIA M., *High-speed optical modulation based on carrier depletion in a silicon waveguide*, Optics Express **15**(2), 2007, pp. 660–668.

[3] FENGNIAN XIA, ROOKS M., SEKARIC L., VLASOV Y., *Ultra-compact high order ring resonator filters using submicron silicon photonic wires for on-chip optical interconnects*, Optics Express **15**(19), 2007, pp. 11934–11941.

[4] YEBO N.A., LOMMENS P., HENS Z., BAETS R., *An integrated optic ethanol vapor sensor based on a silicon-on-insulator microring resonator coated with a porous ZnO film*, Optics Express **18**(11) 2010, pp. 11859–11866.

[5] YARIV A., YEH P., *Optical Wave in Crystals*, John Wiley & Sons, Canada, 2003.

[6] CHIH-MING LIN, WEI-CHENG LIEN, FELMETSGER V.V., HOPCROFT M.A., SENESKY D.G., PISANO A.P., *AlN thin films grown on epitaxial 3C–SiC (100) for piezoelectric resonant devices*, Applied Physics Letters **97**(14), 2010, article 141907.

[7] FENG-CHIA HSU, JIN-CHEN HSU, TSUN-CHE HUANG, CHIN-HUNG WANG, PIN CHANG, *Design of lossless anchors for microacoustic-wave resonators utilizing phononic crystal strips*, Applied Physics Letters **98**(14), 2011, article 143505.

[8] KUZNETSOV S.V., *Lamb waves in anisotropic plates (review)*, Acoustical Physics **60**(1), 2014, pp. 95–103.

[9] CAMPBELL M., SHARP D.N., HARRISON M.T., DENNING R.G., TURBERFIELD A.J., *Fabrication of photonic crystals for the visible spectrum by holographic lithography*, Nature **404**(6773), 2000, p. 53.

[10] ÖZBAY E., MICHEL E., TUTTLE G., BISWAS R., SIGALAS M., HO K.-M., *Micromachined millimeter-wave photonic band-gap crystals*, Applied Physics Letters **64**(16), 1994, p. 2059.

[11] HOWELL I.R., CHENG LI, COLELLA N.S., ITO K., WATKINS J.J., *Strain-tunable one dimensional photonic crystals based on zirconium dioxide/slide-ring elastomer nanocomposites for mechanochromic sensing*, ACS Applied Materials and Interfaces **7**(6), 2015, pp. 3641–3646.

[12] ISHIKAWA Y., WADA K., CANNON D.D., JIFENG LIU, HSIN-CHIAO LUAN, KIMERLING L.C., *Strain-induced band gap shrinkage in Ge grown on Si substrate*, Applied Physics Letters **82**(13), 2003, pp. 2044–2046.

[13] Mᴜɴɢᴜíᴀ J., Bʀᴇᴍᴏɴᴅ G., Bʟᴜᴇᴛ J.M., Hᴀʀᴛᴍᴀɴɴ J.M., Mᴇʀᴍᴏᴜx M., *Strain dependence of indirect band gap for strained silicon on insulator wafers*, Applied Physics Letters **93**(10), 2008, article 102101.

[14] Lᴀᴘɪɴ A.D., *Reflection of Lamb waves in a solid layer by a grating formed by mechanical resonators*, Acoustical Physics **59**(3), 2013, pp. 267–271.

[15] Tᴇʏssɪᴇʀ J., Sᴀᴇɴᴋᴏ S.V., ᴠᴀɴ ᴅᴇʀ Mᴀʀᴇʟ D., Mɪʟɪɴᴋᴏᴠɪᴛᴄʜ M.C., *Photonic crystals cause active colour change in chameleons*, Nature Communications **6**, 2015, article 6368.

[16] Sᴏʀᴇғ R., *Mid-infrared photonics in silicon and germanium*, Nature Photonics **4**(8), 2010, pp. 495–497.

[17] Jɪɴ-Cʜᴇɴ Hsᴜ, Cʜɪᴀɴɢ-Hsɪɴ Lɪɴ, Yᴜɴ-Cʜᴇɴɢ Kᴜ, Tᴢʏ-Rᴏɴɢ Lɪɴ, *Photonic band gaps induced by sub-micron acoustic plate waves in dielectric slab waveguides*, Optics Letters **38**(20), 2013, pp. 4050–4053.

[18] Tᴢʏ-Rᴏɴɢ Lɪɴ, Cʜɪᴀɴɢ-Hsɪɴ Lɪ, Jɪɴ-Cʜᴇɴ Hsᴜ, *Enhanced acousto-optic interaction in two-dimensional phoxonic crystals with a line defect*, Journal of Applied Physics **113**(5), 2013, article 053508.

[19] Rᴏʏᴇʀ D., Dɪᴇᴜʟᴇsᴀɪɴᴛ E., *Elastic Waves in Solids I, Free and Guided Propagation*, Springer-Verlag, Berlin, Heidelberg, 2000.

[20] Mᴀᴋᴏᴠ Yᴜ.N., *Dispersive solutions of the linear wave equation for a nonabsorbing dispersion-free unbounded medium*, Acoustical Physics **58**(1), 2012, pp. 34–40.